Transport and dynamic properties of $O_2^+(X^2\Pi_g)$ in Kr under the action of an electrostatic field: Single or multiple potential energy surface treatment

Andreas D. Koutselos[a)]
Physical Chemistry Laboratory, Department of Chemistry, National and Kapodistrian University of Athens, Panepistimiopolis, 15771 Athens, Greece

(Received 23 February 2011; accepted 19 April 2011; published online 16 May 2011)

Ion transport and dynamic properties are calculated through molecular dynamics simulation of the motion of O_2^+ in Kr under the action of an electrostatic field. The two lower potential energy surfaces $\tilde{X}^2A''$ and $\tilde{A}^2A'$ are considered for the interaction of the Π ground state of the ion with a closed shell noble gas. First, we study the reproduction of experimental mobility data through the use of single and multiple potential energy surfaces and establish the contribution of both lower energy states to the interactions. Further, we obtain mean energies and components of the diffusion coefficient parallel and perpendicular to the field, the latter through calculation of the velocity correlation functions. We also calculate components of the angular momentum which provide a measure of the collisional rotational alignment of the ions at high field strength. © *2011 American Institute of Physics*. [doi:10.1063/1.3589164]

I. INTRODUCTION

The transport properties of ions in a dilute gas under the action of an electrostatic field are controlled by binary collisions and because of this they are studied for their connection to the ion-neutral interaction potential. Kinetic theory calculations of mobility and ion diffusion coefficient components parallel and perpendicular to the field have been employed for testing of proposed interaction potentials through comparison against experimental data,[1–4] or to predict new ones through direct inversion of measured transport coefficients.[5,6] Similarly, a stochastic (Monte-Carlo) nonequilibrium simulation method has been used for evaluation of the performance of different potential models to predict transport properties of atomic systems.[7]

Additional properties sensitive to the collision properties that are measured occasionally are mean kinetic energies parallel and perpendicular to the field, third and fourth order moments of the velocity distribution (v-distribution), as well as, a rotational alignment parameter.[8–10] Such properties are important in gas discharges,[11] upper atmospheric studies,[12] and drift tube experiments.[13] In the case of molecular systems, not only the mean properties but also the ion dynamics have been reproduced most easily through a molecular dynamics (MD) simulation method[14–17] that samples properly the initial ion-neutral collision states at nonequilibrium conditions.

In the following we consider this method in order to study the reproduction of experimental mobility of O_2^+ $(X^2\Pi_g)$ in Kr and compare the use of a single (ground state A'') or multiple (two lower states A'' and A') potential energy surfaces (PES) obtained recently from an accurate *ab initio* quantum molecular calculation by Papakondylis.[18] The system has been studied primarily for the vibrational relaxation[19–24] and transport properties[24] of O_2^+ in Kr and information about the ion-atom interaction has been accumulated through various approaches in the past. Such approaches include experimental estimation of the energy minimum,[25] model calculations,[19–22,26] and an *ab initio* calculation of several adiabatic potential energy surfaces based on a projected valence bond configuration interaction method.[27]

When open shell systems are involved, a number of adiabatic states contribute to the ion motion and usually in kinetic theory calculations a weighted average is considered over their degeneracy and statistical contribution of the corresponding adiabatic potentials.[28] In a similar way, in order to simulate the motion of open shell ions in low density gases by a MD method, we can consider multiple potential energy surfaces with the system hopping between them according to a prescribed rule. Though semiempirical classical trajectory surface-hopping methods[29] produce transition probabilities continuously in time through evolution of the electronic wavefunction, in cases where adiabatic PES lie considerably far apart and they approach one another only at long distance, the hopping could be weighed at the beginning of an ion-atom encounter. With this prescription we calculate transport properties for the ions and compare the results against experimental data.

Further, we obtain mean kinetic energies parallel and perpendicular to the field, as well as the mean rotational orientation of the ions as a function of the field strength. In addition, we calculate velocity correlation functions (v-c functions) and study their form and differences in the cases of using single and multiple PES. Finally, the integration of these v-c functions over time produces diffusion coefficient components parallel and perpendicular to the field.

II. METHOD

The molecular dynamics method that we employ calculates trajectories of ions moving under the action of a homogeneous electrostatic field and interacting continuously with neutral particles of a low density gas that remains always in equilibrium.[15,16] The stationary motion is reached

a)Electronic mail: akoutsel@chem.uoa.gr.

through interaction of the ions not with the (actual) gas atoms but with their images created during an ion-atom encounter. This effective procedure is necessary in order to avoid introduction of effective forces for the energy control of the ions, as in the case of traditional temperature control approaches, since that would disturb the ion motion which is sensitive to the ion-neutral intermolecular potential. The approach allows extension of equilibrium microcanonical MD methods[30,31] to nonequilibrium conditions allowing the use of periodic boundary conditions and the minimum image convention. Here, the translational motion and rotation of the diatomic ion are followed with six- and five-value Nordsieck-Gear predictor-corrector algorithms,[32] respectively.

Given an ion-atom potential surface, V(r, θ), as a function of the distance of the species, r, which is the measure of the vector that connects the atom to the center of mass of the ion, $\vec{r}$, and of the angle, θ, between $\vec{r}$ and the vector along the intermolecular axis of the ion, $\vec{e}$, the force, $\vec{F}$, and torque, t_{ij}, exerted on the ion are given by

$$\vec{F} = -\frac{\vec{r}}{r}\frac{\partial V}{\partial r} - \left(\frac{\vec{e}}{r} - \vec{r}\frac{\cos(\theta)}{r^2}\right)\frac{\partial V}{\partial \cos(\theta)}, \quad (1)$$

$$t_{ij} = -\vec{e} \otimes \frac{\vec{r}}{r}\frac{\partial V}{\partial \cos(\theta)}, \quad (2)$$

and similarly the force on the gas atom is $-\vec{F}$. The two derivative terms, $(1/r)\partial V/\partial r$ and $(1/r)\partial V/\partial\cos(\theta)$, which are required, have to be calculated for both A″ and A′ potential energy surfaces. The latter have been produced in terms of a coarse grained grid defined by a set of 30×7, (r_i, θ_i), points.[18] In order to make certain the smooth interpolation and accurate calculation of the derivative quantities, we calculate and store their values over a fine grid of 100×90 points. In general, interpolation methods introduce discontinuities at coarse grid points whenever derivatives are calculated. For this reason, we interpolated first the potential along the r variable at certain (coarse) θ_i points and then the obtained $V(r_i, \theta_i)$ along the θ variable at all fine r_i points using an extended second order method (Appendix). During the simulation run the forces and torques at instantaneous (r, θ) values are calculated from a two-dimensional linear interpolation of the fine grid values of the potential energy derivatives. The slowing down during retrieval of these values from the memory of the computer is compensated by the use of parallel implementation of the program code. In each computing process we simulate the motion of 130 ions, independent from one another, in 108 neutrals.

The distance variable is defined from a short-distance cutoff, $r_s = 2.00$ Å, up to a long-distance cutoff, $r_p = 6.50$ Å, and the angle runs from 0° to 90°. Although the potential at small r is quite high and repels the interacting species, we take provision at $r < r_s$ for the forces to be calculated directly from a r^{-12} potential function fitted to the values of potential surfaces around the short-range limit. At long distance all *ab initio* potential data converge to the polarization potential, $-a_d/2r^4$, where a_d is the dipole polarizability of Kr, $a_d = 16.74\, a_0{}^3$.[33] Thus, to increase the accuracy and efficiency at long distance we follow the analytic form of the polarization potential beyond r_p and restrict the use of grid at shorter distances. The evolution of the rotational motion requires the use of the moment of inertia of $O_2{}^+$ and this is determined by the internuclear separation which is set equal to the experimental value of 1.117 Å.[34]

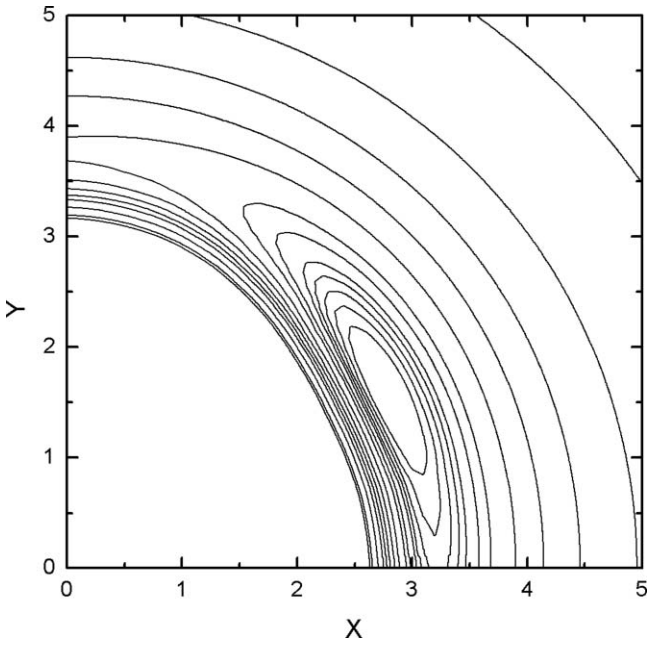

FIG. 1. Contour plot of the mean potential energy surface of the A″ and A′ states. The O-O axis lies in the y axis with the origin set at the center of the molecule. The axes are in units of Å.

The ion-atom interactions are introduced through various PES in order to examine their role in determining the ion properties under the action of an electrostatic field. Thus, we examine the reproduction of mobility through use of the potentials of the ground state A″, the simultaneous use of both A″ and first exited A′ states with 50% probability each, as well as, the A′ state alone for comparison. However, at low density conditions of the present MD conditions, where binary uncorrelated collisions prevail, the use of the above multiple potential energy surfaces may not differ from the use of the mean PES, $V_m = (V_{A''} + V_{A'})/2$, where V_X is the potential surface of state X. To examine this expectation we have calculated in addition all the ion properties by using the V_m potential surface, Fig. 1, at certain field strengths that represent the weak, intermediate, and high field regions. The interactions between the Kr atoms are assumed to follow a Lennard-Jones potential[35] that reproduces accurately equilibrium properties and its functional form is implemented most efficiently in the computation.

Statistical averages were obtained during several million collisions after both the gas and the ions had relaxed to a steady state at certain field strength, E, and gas temperature, T = 300 K. At the low density drift tube experimental conditions, which are followed in the simulation procedure, the ion properties depend on the combined parameter E/N,[13] where N is the gas number density, reported in units of Td, with 1 Td = 10^{-17} Vcm^2. The mobility, K, is calculated through $K = v_d/E$, where v_d is the mean ion velocity, $v_d = \langle v_z \rangle$ with the field in the z-direction. The mean kinetic energies parallel and perpendicular to the field are expressed as

effective temperatures through

$$\frac{1}{2}kT_x = \frac{1}{2}m\langle(v_x - \langle v_x\rangle)^2\rangle, \quad (3)$$

$$\frac{1}{2}kT_y = \frac{1}{2}m\langle(v_y - \langle v_y\rangle)^2\rangle, \quad (4)$$

$$\frac{1}{2}kT_z = \frac{1}{2}m\langle(v_z - \langle v_z\rangle)^2\rangle, \quad (5)$$

where m is the mass of the ion. At each time step, the ensemble averages produce $\langle v_x\rangle \approx \langle v_y\rangle \approx 0$ and $\langle v_z\rangle \approx v_d$. We mention that the cylindrical symmetry of the mean motion dictates $\langle(v_x - \langle v_x\rangle)^2\rangle = \langle(v_y - \langle v_y\rangle)^2\rangle$, which is also approximately followed at each time-step of the procedure. Only at the end of the computation do time averages approach the macroscopic limit with vanishing uncertainty and then we can set $T_\parallel = T_z$ and $T_\perp = (T_x + T_y)/2$. From these temperatures the total effective translation temperature is calculated through

$$\frac{3}{2}kT_{trl} = \frac{1}{2}kT_\parallel + kT_\perp. \quad (6)$$

In analogy, the mean rotation energy is given by

$$\frac{1}{2}kT_{r,x} = \frac{1}{2}I_x\langle(w_x - \langle w_x\rangle)^2\rangle, \quad (7)$$

$$\frac{1}{2}kT_{r,y} = \frac{1}{2}I_y\langle(w_y - \langle w_y\rangle)^2\rangle, \quad (8)$$

with the angular velocity and the moment of inertia defined relative to a body coordinate system at the center of mass of the ion. The x and y coordinates are considered perpendicular to the molecular axis. Due to the molecular symmetry, the x and y components of the above quantities are equal to one another and therefore $T_{r,x} = T_{r,y}$. The total rotation effective temperature is calculated through

$$T_r = \frac{1}{2}(T_{r,x} + T_{r,y}). \quad (9)$$

The components of the diffusion coefficient are obtained through the use of the v-c functions,

$$D_{ii} = \int_0^\infty C_{ii}(t)dt, \quad (10)$$

where i represents {x, y, z} directions. The correlation function components are defined through

$$C_{ii} = \langle(v_i(0) - \langle v_i(0)\rangle)(v_i(t) - \langle v_i(t)\rangle)\rangle. \quad (11)$$

The cross terms vanish and from the diagonal elements the perpendicular components should be equal to one another, $C_{xx} = C_{yy,}$. In addition, the steady conditions obtained through the MD procedure produce $\langle v_i(0)\rangle = \langle v_i(t)\rangle$. Similarly, in the case of the diffusion coefficients only the diagonal components do not vanish and at the end of the computation we calculate $D_\parallel = D_z$ and $D_\perp = (D_x + D_y)/2$. This procedure is based on the hypothesis that the regression of local density fluctuations from a homogeneous steady state during the ion motion follows the macroscopic transport equations,[36] which should be consistent with the low density drift tube experimental conditions where binary uncorrelated ion-neutral collision take place and ions move independently from one another. In cases where correlations may develop in denser systems and at strong fields the obtained "theoretical" diffusion coefficients may not coincide with the experimental ones.[37,38]

Finally, the rotational alignment of the ion is studied through calculation of a quadrupole alignment parameter[10,39] from the components of the angular momentum, L_i, defined in a laboratory frame,

$$A_0^{(2)} = 3\langle\hat{L}_z^2\rangle - 1, \quad (12)$$

where $\langle\hat{L}_z^2\rangle$ is the square of the z-component of a unit angular momentum calculated here through $\langle L_z^2\rangle/(\langle L_x^2\rangle + \langle L_y^2\rangle + \langle L_z^2\rangle$. At weak fields $A_0{}^{(2)}$ vanishes due to the spherical symmetry of the motion, but at strong fields the collision may favor other values depending on the nonequilibrium weighting of the scattering conditions.

III. RESULTS

The potential energy surfaces of the two lower $\tilde{X}^2A''$ and $\tilde{A}^2A'$ states of KrO_2^+ have been calculated recently through an accurate *ab initio* RCCSD(T) calculation[18] and we employ them here for the reproduction of transport and dynamic properties of the O_2^+ in Kr at the whole experimental field range. It has been found that the ground state, with the aug-cc-pVQZ basis set, acquires a rather deep asymmetric minimum for a non-bonded system, of 0.230 eV depth, at distance r_m = 2.996 Å and angle between Kr and the center of mass of O_2^+ of 125.9°. The obtained well depth is at the edge of experimental uncertainty of 0.33 ± 0.1 eV estimated by photodissociation data of Jarrold *et al.*[25] It was attributed to a weak "chemical" character of the bonding that was due to a weak charge transfer from Kr to the in-plane π_g orbital of O_2^+. The *ab initio* first excited state was found, at the same level of accuracy, to have also a T-shaped symmetric minimum at r_m = 3.264 Å of a reasonable depth of 0.137 eV. These adiabatic surfaces do not intersect and approach the same limit at infinity characterized by the $X\,^2\Pi_g$ state of O_2^+ and ^1S state of Kr. For this reason, when we assume that both surfaces contribute to the ion-atom interaction, they are sampled with the same rate during the MD simulation. In the past another *ab initio* calculation procedure with a relatively small basis sets was utilized by Ramiro-Diaz *et al.*[27] for the determination of the potential surfaces of several similar states. The ground state acquired weaker minimum with binding energy 0.173 eV. The remaining states, including the first excited one, were found to be strictly repulsive. The PES of the lower states have been used in vibration relaxation studies in the past and have been found not to reproduce well the relaxation rates as a function of the ion-neutral collision energy.[23] Even though the disagreement is partially due to the employed scattering methods, it appears that these PES are of limited accuracy and therefore we do not employ them here. Later we

TABLE I. Molecular dynamics simulation results for O_2^+ in Kr at 300 K through multiple potential energy surface treatment.

E/N (Td)	K_0 (cm^2/Vs)	$T_\parallel$ (K)	$T_\perp$ (K)	T_r (K)	T_r/T_{trl}[a]	$A_0^{(2)}*10^3$[b]	$ND_\parallel$ (10^{18}/cm s)	$ND_\perp$ (10^{18}/cm s)
10	1.799	319.4	314.3	318.7	1.009	− 1.96	1.24	1.28
20	1.778	352.6	335.9	342.1	1.002	1.79	1.36	1.40
40	1.853	485.3	421.0	428.9	0.969	− 0.632	1.76	1.87
60	2.048	810.7	642.8	693.1	0.992	− 1.93	3.10	4.19
80	2.275	1388	1031	1111	0.966	− 5.91	5.46	8.09
100	2.367	2108	1560	1787	1.025	− 6.60	8.90	12.80
120	2.454	2948	2176	2608	1.072	− 5.50	12.31	17.13
170	2.431	5236	3964	5063	1.154	− 5.26	22.54	28.02

[a]Ratio of rotational to translational effective temperatures.
[b]Alignment parameter $A_0^{(2)}$ of Eq. (12).

comment on the reproduction of the experimental mobility from the ground state of this approach.

The deep minimum of the ground state requires the use of high molar volume, v_m, for the Kr gas (around $v_m = 0.08$ m^3) during the computation, in order to avoid clustering at weak fields (E/N < 20 Td), especially due to the occurrence of long collision lifetime in addition to strong attractive forces. At stronger field strengths the density can be increased, with v_m around 0.04 m^3, in order for the method to become more efficient due to the increase of the ion-atom collision rate. Further, the asymmetry and the attractiveness of the ground state potential function excites the rotation of O_2^+ requiring very small integration time steps of the order of 2×10^{-17} s. This effect was identified from the high rotational energy of the ions which was found to accumulate even at weak fields when the ground state PES was contributing to the interaction. Only at such small time-steps does the rotational temperature approach the translation temperature as a limiting value. To avoid uncontrolled energy exchange, the same condition was used in all cases, even when the exited shallow symmetric PES was involved in the computation.

The results are obtained at a third stage of the procedure, after the neutrals and the ions have reached steady motion and after several million collisions have taken place. The transport properties that have been calculated from the multiple PES are summarized in Table I. The ion mobility using single and multiple PES is presented in Fig. 2, together with experimental data of ±6% error bars.[40] It has been converted to standard mobility at standard gas conditions through $K_0 = (p/760)(273.15/T)K$, where p is the gas pressure in torr. The convergence of the results of the current method is within a few percent at weak fields and around 1% at intermediate and strong fields. We observe that the mobility from a single PES, of A″ or A′ states, remain at the edge of the experimental accuracy and that the multiple potential treatment reproduces well the measured mobility. In addition, we are presenting the mobility obtained from the use of the mean potential, V_m, at certain field strengths, (40 Td, 100 Td, and 170 Td), that cover the whole experimental field range. These results lie very close to those of the multiple potential as one would expect due to the fact that the subsequent ion-atom collisions are uncorrelated. However, it is not obvious that the same will hold in the case of the dynamic properties, especially since the mean potential acquires different form from both PES of A″ and A′ states.

We mention here that in the past various model potential functions have been used for the description of the interaction of this system and two recent ones have been found to reproduce accurately the mobility data as well. In a vibration relaxation study a site-site 12-6-4 potential was employed with minimum around the asymmetric minimum of the ground state potential surface of Ramiro-Diaz *et al.*[27] of depth 0.173 eV at $r_m = 3.10$ Å, and recently a spherical Morse-Morse-Spline-van der Waals interaction potential was determined that reproduces most accurately the mobility data with depth 0.1255 eV at $r_m = 3.462$ Å.[26] Thus, it becomes apparent that though inversion of mobility data, which can by now be measured accurately within 1%, can produce reliable interaction potential functions in the case of atomic systems,[5,6] it may not produce accurate PES in the case of molecular systems. In the latter case, other experimental information such as diffusion coefficient components, spectroscopic and scattering data can assist in the determination of the ion-neutral PES. The similarity of the behavior of the above model potential functions, however, should be attributed to the fact that the

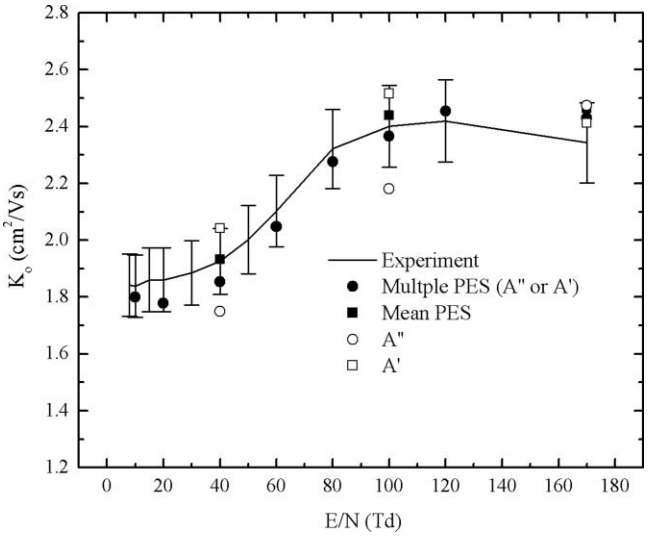

FIG. 2. Calculated and experimental standard mobility at 300 K as a function of the ratio of the electric field strength to the gas number density. The solid line represents measured mobility with ±6% error bars and the remaining data are results of the present method, with filled circles obtained from the use of multiple PES, filled squares from the mean PES, and open circles and squares were derived from the single A″ and A′ states, respectively.

long range part of the potential is similar, determined mainly by the polarization limit, $-a_d/2r^4$, and that the depths and the positions of the minima of the above model potentials are not very different from the depth, 0.165 eV, and the position, r_m = 3.213 Å, of the minimum of the mean PES used here, Fig. 1. Despite this, the comparison of calculated mobility coefficients against experimental ones provides a test for the reliability of the employed ion-atom potential surfaces, and therefore the performance of the two lower energy *ab initio* PES of Papakondylis[18] in reproducing the experimental mobility and the high approximation involved in their determination indicate that these PES should be considered as describing the O_2^+-Kr interactions quite accurately and in more detail than any other so far. The latter, especially since the ground state PES acquires an asymmetric minimum close to the one estimated through photodissociation experiments of O_2^+-Kr cluster.

The obtained mean kinetic energies expressed as effective temperatures through Eqs. (3)–(5) for the multiple and mean potential cases are presented in Fig. 3(a). The results in both cases lie close to one another at all field strengths. In addition, we compare the rotational (internal) energy of the ions, kT_r, with the relative kinetic energy defined in the ion-neutral center of mass, ε, which are expected to be equal to one another in the case of molecular ions in atomic gases, as predicted from momentum transfer theory and low approximation of kinetic theory results.[41,42] In this comparison we employ the use of multiple PES. A simple representation of the relative collision kinetic energy, which has been used in the interpretation of laser fluorescence experiments in the case of molecular ion systems,[43,44] is given by the Wannier expression,[42]

$$\varepsilon_W = \frac{3}{2}kT + \frac{1}{2}Mv_d^2 \equiv kT_{eff}, \tag{13}$$

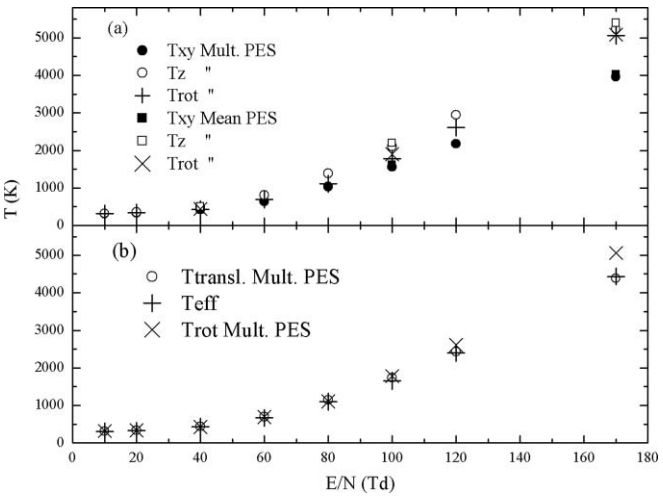

FIG. 3. (a) Filled and open circles are translational temperatures perpendicular and parallel to the field, crosses depict the rotational temperature, all calculated with multiple PES. Filled and open squares are translation temperatures perpendicular and parallel to the field, sidelong crosses represent the rotational temperature, all obtained from the mean PES. (b) Open circle and sidelong crosses are total translation and rotation temperatures, (Eqs. (14) and (9), respectively) from the multiple PES. Crosses are effective temperatures of Wannier energy, Eq. (13).

where M is the mass of the neutral, and from which the effective temperature T_{eff} is defined. However, since within the Wannier[42] approach ε_W can also be expressed as

$$\varepsilon_W = \frac{3}{2}kT_{trl} = \frac{1}{2}kT_{\parallel} + kT_{\perp}, \tag{14}$$

there are two independent ways to estimate ε from quantities calculated through the MD simulation. We thus compare first the corresponding effective temperatures, T_{trl} and T_{eff} calculated through Eqs. (6) and (13), Fig. 3(b), and find that they remain close to one another within the calculation error which is a few percent in the whole range of field strengths. Further, both these quantities are found to agree well to the rotation effective temperature, T_r, at low field strengths and to develop differences up to 10% at strong fields, beyond the calculation error, Table I. Such deviations should be explained by more elaborate expressions for ε obtained from the analytic solution of a generalized Boltzmann kinetic equation for inelastic ion-atom systems.[41,45]

A similar behavior between the results for the two potential energy surface cases is observed also in the calculation of the quadrupole alignment parameter, $A_0^{(2)}$, defined in Eq. (12), which is presented in Fig. 4 in terms of the field strength. It becomes apparent that the collisions of O_2^+ with Kr at high field strengths decrease the value of $A_0^{(2)}$ and induce angular orientation to the ion. Since $A_0^{(2)}$ of Eq. (12) can be written as

$$A_0^{(2)} = 2\langle L_z^2 - L_\perp^2 \rangle / \langle L^2 \rangle, \tag{15}$$

where $L^2 = L_x^2 + L_y^2 + L_z^2$ and $\langle L_\perp^2 \rangle = \langle L_x^2 \rangle = \langle L_y^2 \rangle$, the perpendicular to the field component of the angular momentum is favored relative to the parallel one. Thus, even by a small amount, the "helicopter" type rotation of the ion is favored relative to the "plane" type rotation, as observed and studied in other ion-neutral systems by molecular dynamics simulations in the past.[17]

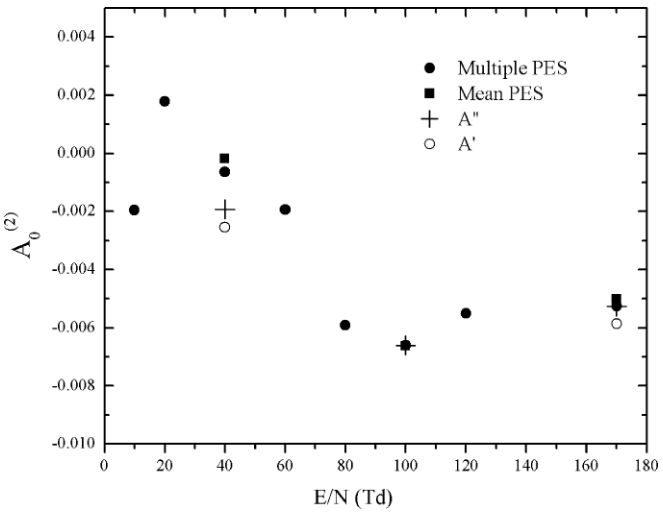

FIG. 4. Alignment parameter $A_0^{(2)}$ as a function of E/N. Filled circles represent results from use of multiple PES, filled squares results from the mean PES, and crosses and open circles results from the A″ and A′ single states, respectively.

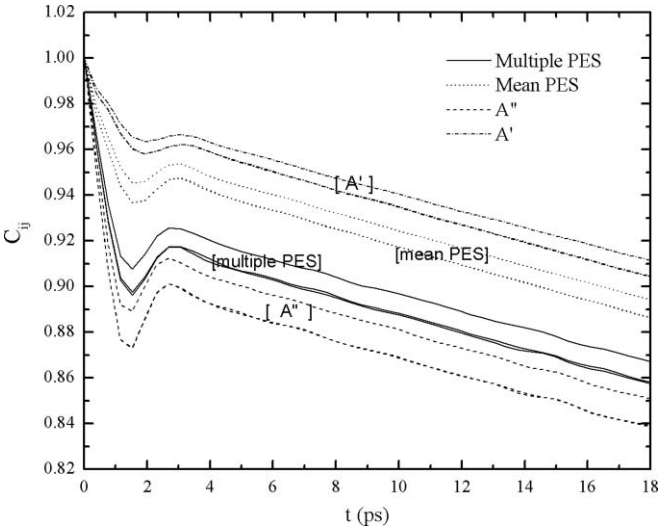

FIG. 5. Velocity correlation functions for various potential surfaces, with the zz component lying above the almost identical xx and yy components. The solid line is obtained from the use of multiple PES, the dotted line from the mean PES, and dashed and dotted-dashed lines are derived from the single A″ and A′ single states, respectively.

Finally, we compare the results of the potential energy surfaces for the velocity correlation function, which as a dynamic property may depend more sensitively to the shape of the potential. In Fig. 5 we present the result for single, multiple, and mean PES at 40 Td. At such low field strengths the differences are exaggerated due to the fact that the v-c function is more sensitive to the form of the sampled potential surface. The perpendicular (xx and yy) components are difficult to be identified because their graphs lie very close to one another, as they should, indicating ample sampling of events during the computation. The obtained correlation functions of the multiple and mean potential cases remain in between the single potential surfaces at all times and their difference produces diffusion coefficient components that differ by about 6%. At higher field strengths the relative difference becomes smaller. Thus, in order to differentiate the performance of these two PES cases most easily, experimental diffusion coefficients of higher than 6% accuracy at weak fields are needed. The correlation function of the A″ state lies below that of the A′ state due to the fact the potential surface is deeper and the stronger ion-atom interactions randomize the motion of the ion faster. Finally, the small deep of the v-c function, that occurs at short times, is primarily due to the partial and complete orbiting (binary) collisions. Exclusion of most of these cases from the calculation led to drastic decrease of the deepening. This feature disappears as the field strength is increased. The components of the diffusion coefficient are obtained from integration of the components of the v-c function, Eq. (10), over two time intervals.[36] A first part is obtained through numerical integration up to about 10 ps, during the third stage of the simulation procedure, and for the second part the v-c function is fitted by a decaying exponential and is integrated up to infinity. All mean values of the calculated properties are collected in Table I.

IV. CONCLUSIONS

The reproduction of experimental mobility data of O_2^+ in Kr as a function of the electric field strength through a molecular dynamics simulation method has shown that both the ground, A″, and first excited, A′, states are needed to participate for the description of the ion-atom interactions. We found that the multiple treatment of the PES of these states obtained from an *ab initio* RCCSD(T) calculation, as well as, the mean PES suffice to reproduce the measured mobility within the experimental uncertainty. After establishing the accuracy of the procedure various mean ion-properties were calculated such as the mean translation kinetic energies, parallel and perpendicular to the field, and the mean rotational energy, all expressed as effective temperatures. The calculated mean translational effective temperature compares well to the rotational temperature at weak fields but these quantities differ considerably, beyond the calculation error, at high field strengths. In addition, the quadrupole alignment parameter based on the components of the angular momentum is obtained that provides information about the rotational alignment of the ions induced by the collisions with the neutrals under the action of the electric field. Finally, diffusion coefficients parallel and perpendicular to the field are calculated through integration of the components of the v-c functions over time.

The comparison of the v-c functions of the various potential surfaces has shown that the results are in conformity to the above general conclusion about the use of PES, and that only at low field strength, below 40 Td, the differences observed between the multiple and mean PES treatment may be resolved, provided the relative experimental error of diffusion data is better than 6%.

ACKNOWLEDGMENTS

The authors would like to thank A. Papakondylis for providing the O_2^+-Kr potential energy surfaces prior to publication and the Computer Center of the National and Kapodistrian University of Athens for the computational support. The work was supported by grants from the Research Fund of the National and Kapodistrian University of Athens (Grant No. 70/4/9496).

APPENDIX: DETAILS OF THE INTERPOLATION METHOD

The interpolation method is based on the calculation of the mean value of two extensions (to the left and to the right) of potential functions on a specific interval. Specifically, for a sequence of x_n grid points and corresponding potential energy values $V_n = V(x_n)$, two second order extensions on the same interval (x_n, x_{n-1}) are considered. The first, $V_{l,n}(x)$, is defined from the potential surface at these points, (V_n, V_{n+1}), and the slope at the left side of the interval, $s_l = (V_n - V_{n-1})/(x_n - x_{n-1})$, and the second, $V_{r,n}(x)$, from the same potential surface values and the slope at the right side of the interval, $s_r = (V_{n+1} - V_n)/(x_{n+1} - x_n)$. Then the interpolation of the potential energy surface between the points (x_n, x_{n-1}) is defined through $V(x) = (V_{l,n}(x) + V_{r,n}(x))/2$. The procedure smoothens the interpolated surface and the first order

derivatives around the connecting x_n points, due to the fact that each slope contributes to the interpolations at two adjacent intervals.

[1] I. R. Gatland, L. A. Viehland, and E. A. Mason, J. Chem. Phys. **66**, 537 (1977).
[2] P-H. Larsen, H. R. Skullerud, T. H. Lovaas, and Th. Stefansson, J. Phys. B **21**, 2519 (1988).
[3] A. A. Buchachenko, R. V. Krems, M. M. Szczesniak, Y.-D. Xiao, L. A. Viehland, and G. Chałasinski, J. Chem. Phys. **114**, 9919 (2001).
[4] D. M. Danailov, L. A. Viehland, R. Johnsen, T. G. Wright, and A. S. Dickinson, J. Chem. Phys. **128**, 134302 (2008).
[5] L. A. Viehland, M. M. Harrington, and E. A. Mason, Chem. Phys. **17**, 433 (1976).
[6] L. A. Viehland, Chem. Phys. **78**, 279 (1983); **85**, 291 (1984).
[7] P. P. Ong and M. J. Hogan, J. Phys. B **24**, 3193 (1991); M. J. Hogan and P. P. Ong, Phys. Rev. A **44**, 1597 (1991).
[8] S. M. Penn, J. P. M. Beijers, R. A. Dressler, V. M. Bierbaum, and S. R. Leone, J. Chem. Phys. **93**, 5118 (1990).
[9] C. P. Lauenstein, M. J. Bastian, V. M. Bierbaum, S. M. Penn, and S. R. Leone, J. Chem. Phys. **94**, 7810 (1991).
[10] E. B. Anthony, V. M. Bierbaum, and S. R. Leone, J. Chem. Phys. **114**, 6654 (2001).
[11] J. Borysow and A. V. Phelps, Phys. Rev. E **50**, 1399 (1994).
[12] A. A. Viggiano, Phys. Chem. Chem. Phys. **8**, 2557 (2006).
[13] E. A. Mason and E. W. McDaniel, *Transport Properties of Ions in Gases* (Wiley, New York, 1988).
[14] A. D. Koutselos, J. Chem. Phys. **102**, 7216 (1995).
[15] G. Balla and A. D. Koutselos, J. Chem. Phys. **119**, 11374 (2003).
[16] A. D. Koutselos and J. Samios, Pure Appl. Chem. **76**, 223 (2004).
[17] X. Chen and M. Thachuk, J. Chem. Phys. **124**, 174501 (2006).
[18] A. Papakondylis, Chem. Phys. Lett. **484**, 165 (2009).
[19] P. Tosi and M. Ronchetti, Chem. Phys. Lett. **136**, 398 (1987); P. Tosi, M. Ronchetti, and A. Lagana, J. Chem. Phys. **88**, 4814 (1988).
[20] G. Ramachandran and G. S. Ezra, J. Chem. Phys. **97**, 6322 (1992).
[21] E. M. Goldfield, J. Chem. Phys. **97**, 1773 (1992).
[22] F. A. Gianturco, S. Serna, A. Palma, G. D. Billing, and V. Zenevich, J. Phys. B **26**, 1839 (1993).
[23] M. Craimer, S. K. Pogrebnya, and D. C. Clary, J. Chem. Phys. **111**, 1972 (1999).
[24] A. D. Koutselos, J. Chem. Phys. **125**, 244304 (2006).
[25] M. F. Jarrold, L. Misev, and M. T. Bowers, J. Chem. Phys. **81**, 4369 (1984).
[26] A. H. Jalili, A. Abbaspour, H. Behnejad, and L. A. Viehland, Mol. Phys. **108**, 35 (2010).
[27] B. Ramiro-Diaz, P. Wahnon, and V. Sidis, J. Chem. Phys. **104**, 191 (1996).
[28] L. A. Viehland, Aust. J. Phys. **50**, 671 (1997).
[29] J. C. Tully, in *Dynamics of Molecular Collisions, Part B*, edited by W. H. Miller (Plenum, New York, 1976), p. 217; A. W. Kleyn, J. Los, and E. A. Gislason, Phys. Rep. **90**, 1 (1982); J. R. Stine and J. T. Muckerman, J. Phys. Chem. **91**, 459 (1987).
[30] M. P. Allen and D. J. Tildesley, *Computer Simulation of Liquids* (Clarendon, Oxford, 1987).
[31] D. C. Rapaport, *The Art of Molecular Dynamics Simulation* (Cambridge University Press, Cambridge, 1995).
[32] A. Nordsieck, Math, Comp. **16**, 22 (1962); C. W. Gear, *Numerical Initial Value Problems in Ordinary Differential Equations* (Prentice-Hall, Englewood Cliffs, NJ, 1971), p. 154.
[33] R. P. Teachout and R. T. Pack, At. Data **3**, 195 (1971).
[34] P. H. Krupenie, J. Phys. Chem. Ref. Data, **1**, 423, (1972).
[35] J. A. Beattie, R. J. Barriault, and J. S. Brierly, J. Chem. Phys. **20**, 1613 (1952).
[36] A. D. Koutselos, J. Chem. Phys. **104**, 8442 (1996).
[37] K. Kumar, H. R. Skullerud, and R. E. Robson, Aust. J. Phys. **33**, 343 (1980).
[38] R. E. Robson, Aust. J. Phys. **45**, 677 (1995).
[39] A. J. Orr-Ewing and R. N. Zare, Ann. Rev. Phys. Chem. **45**, 315 (1994).
[40] Y. Kondo and J. L. Moruzzi, Int. J. Mass Spectrom. Ion Phys. **38**, 1 (1981).
[41] L. A. Viehland, S. L. Lin, and E. A. Mason, Chem. Phys. **54**, 341 (1981).
[42] L. A. Viehland and R. E. Robson, Int. J. Mass Spectrom. Ion Process. **90**, 167 (1989).
[43] M. A. Duncan, V. M. Bierbaum, G. Barney, and S. R. Leone, J. Chem. Phys. **79**, 5448 (1983).
[44] W. Lindinger, Int. J. Mass Spectrom. Ion Process. **80**, 115 (1987).
[45] A. D. Koutselos and E. A. Mason, Chem. Phys. **153**, 351 (1991).